Czech Technical University in Prague
Faculty of Mechanical Engineering

Summary of Dissertation Thesis

Numerical Solution of Steady and Unsteady Compressible Flow

Petr Furmánek

Doctoral Degree Programme
Mathematical and Physical Engineering

Supervisor
Prof. RNDr. Karel Kozel, DrSc.

2008 Praha

This doctoral thesis is an outcome of a full-time doctoral study programme at the Departament of Technical Mathematics, Faculty of Mechanical Engineering, Czech Technical University in Prague.

Doctoral Degree Programme: Mathematical and Physical Engineering

Disertant: Ing. Petr Furmánek

Supervisor: Prof. RNDr. Karel Kozel, DrSc.

Opponents:
Prof. Ing. Jaroslav Fořt, CSc., ČVUT v Praze, Fakulta strojní
Prof. Ing. Pavel Šafařík, CSc., ČAV, Ústav termomechaniky
Ing. Milan Kladrubský, VZLÚ a. s.
The thesis was set out on:

The defense of the dissertation thesis will take place on:
in the room 104 Faculty of Mechanical Engineering, Karlovo náměstí 13, 12135, Praha 2 - Nové Město, in front of the ad hoc commitee in the study programme Mathematical and Physical Engineering. The thesis is available in the Department od Science and Research of Faculty of Mechanical Engineering, CTU in Prague, Technická 4, Praha 6 - Dejvice.

Prof. RNDr. Karel Kozel, DrSc.
Head of Doctoral Study Programme
Mathematical and Physical Engineering
Czech Technical University in Prague
Faculty of Mechanical Engineering

Summary

The aim of this thesis is to develop and implement various numerical methods suitable for solution of three-dimmensional unsteady compressible transonic inviscid flow. The mathematical model describing the mentioned problem is derived with the use of the basic conservation laws in the first part of the thesis. At first only the steady state with adequate boundary conditions is considered. Then the Arbitrary Lagrangian-Eulerian method and Small Disturbance theory are used for description of unsteady flows. Various numerical FVM schemes are proposed in the second part. The emphasis is placed on their ability to capture important flow characteristics. Because the considered case is transonic and unsteady, it is characterized by the occurance of shock waves, which may be interpreted as discontinuities in the physical quantities used for flow description. In order to simulate them correctly, some high-order schemes are constructed. Obtained numerical results are successfuly compared with numerical results of other authors and also experimental data from IT CAS, AGARD and ONERA for both steady and unsteady cases.

Shrnutí

Cílem této disertační práce bylo navrhnout a implementovat numerické metody pro řešení 2D a 3D stacionárního a nestacionárního transsonického stlačitelného proudění ve vnější aerodynamice. V první části je pomocí základních zákonů zachování odvozen matematický model vhodný pro popis uvažovaných případů proudění. Při jeho odvozování je nejprve uveden stacionárni stav (spolu s odpovídajícími okrajovými podmínkami), který je posléze pomocí metod SDT a ALE rozšíren i na nestacionární případy. Druhá část je věnována návrhu numerických schemat metody konečných objemů (FVM) schopných zachytit důležité charakteristiky proudění ve zkoumaných případech. Uvažovaný režim je převážně transsonický a nestacionární a je tedy charakterizován mimo jiné výskytem tzv. rázových vln, které lze interpretovat jako nespojitosti v rozložení veličin popisujících proudění. Proto byla pro numerickou simulaci vybrána schemata vyššího řádu přesnosti v prostoru a čase. Odvozené metody jsou otestovány jak na stacionárních tak nestacionárních případech dvou- a třírozmerného proudění pro různé typy profilů a křídel. Získané výsledky jsou v dobré shodě s výsledky jiných autorů a experimentálními daty naměřenými na ústavech ÚT ČAV, AGARD a ONERA.

List of Symbols

Alphanumeric Symbols

c [m]	Profile chord length
c_{ij}	Local sound-speed, 2D
c_p	Pressure coefficient
c_n	Lift coefficient
e	Energy
f [Hz]	Frequency
k [Hz]	Reduced frequency
$\mathbf{n}$	Unit normal vector
p [Pa]	Dynamic pressure
t [s]	Time
Δt [s]	Time step
(u, v, w) [m s^{-1}]	Velocity vector components
x, y, z [m]	Spatial coordinates
x_{ref}	Reference point
w_i	i-th component of domain velocity
$\mathbf{w}$	Domain (grid) velocity
$\mathbf{F}, \mathbf{G}, \mathbf{H}$	Flux vectors
F^c, G^c, H^c	Convective flux vectors
$\mathbf{F}^v$, $\mathbf{G}^v, \mathbf{H}^v$	Diffusive flux vectors
M	Mach number
Pr	Prandtl number
Re	Reynolds number
T [K]	Temperature
T	Nondimensional temperature
$\mathbf{W}$	Vector of conservative variables
∂D_i	Boundary of the finite volume cell D_i
$\lvert D_i \rvert$	Volume (area) of the finite volume cell D_i

Greek Symbols

α_1, α_2	Angle of attack
$\alpha_1(\mathsf{t})$	Pitching angle

Γ	Boundary of a solution domain Ω
η $[\mathrm{m}^2\ \mathrm{s}^{-1}]$	Coefficient of viscosity (dynamical viscosity)
ϕ_0 [rad]	Initial deviation angle
ϕ_1 [rad]	Maximal amplitude
κ	Gas constant
ρ $[\mathrm{kg}\ \mathrm{m}^{-3}]$	Mass density
τ_{ij} $[\mathrm{m}^2\ \mathrm{s}^{-2}]$	ij-th component of tensor of viscous stresses
ω $[\mathrm{rad} \cdot \mathrm{sec}^{-1}]$	Angular velocity

Contents

Introduction

Non-steady flows with aeroelastic effects appear in many physical processes of fluid dynamics including turbomachinery flows, flows in the atmosphere boundary layer, blood flow and last but not least in wing deformations during high-speed flight. The proper wing design is crucial for achievement of desired flight characteristics of all transonic (and potentially hypersonic) public, commercial and military freighters and fighter-planes. In the pioneer years of supersonic flights the unsteady effects often led even to the destruction of a wing designed for subsonic flights and therefore experiencing destructive oscillations during the transition from subsonic into supersonic flight. Although this problem has been solved a long time ago, new problems emerge constantly with the use and discovery of new materials and procedures in airplanes construction. Therefore the numerical simulations of mentioned effects have become an important way in their investigation because they allow consideration of such flow regimes that would have catastrophic consequences in reality.

The aim of this thesis is to numerically investigate behaviour of transonic inviscid flow over an airfoil and a wing, respectively, considering forced oscillatory motion. In the first part the governing systems of equations are discussed. These are the system of Euler equation describing the flow of 3D compressible inviscid flow and the system of Navier-Stokes equation describing flow of 3D viscous compressible fluid. The boundary condition for the case of general 3D system of Euler equations are shown and one of the possible ways of choosing the boundary conditions for Navier-Stokes equations is also presented. Since no analytical solution of mentioned systems has been discovered till today, the last chapter of the first part contains one of possible approaches of so called *weak* solution definition, on the base of which the numerical solution is derived.

The second part is devoted to numerical methods used for numerical solution. Further, two methods suitable for solution of 3D unsteady problems are introduced. Namely the Small Disturbance Theory and Arbitrary Lagrangian-Eulerian method. The mathematical background of these methods is presented and the mentioned schemes are extended into the "unsteady" form. The penultimate chapter deals with the governing equation of profile motion and geometry change during the unsteady computations. Properties of computational meshes for both steady and unsteady flows are described in the last chapter.

Numerical results achieved by the author and their comparison both with

experimental data and numerical results of other authors form the contents of the third part, which is divided in two chapters. The first contains the results of simulation of steady inviscid and laminar flows and the second deals with the unsteady simulation of inviscid flows. Both 2D and 3D subsonic and transonic flows are considered.

State of the Art

In present days there are generally available two ways of numerical investigation of unsteady flows (as for example flow around an oscillating wing - either with forced oscillatory motion or experiencing aeroelastic effects due to flutter). The first is use of some of the commercial software packages as FLUENT, ANSYS CFX, NASTRAN or STAR-CD which are however able to handle only particular unsteady problems of aeroelasticity or hydroelasticity and are limited mainly to linearised models. When a need for investigation of more complex problems arise simulation of the particular problem with a self-implemented method can be the second option. The advantage of this approach is better adaptation of the chosen method to the problem and also the inconsiderable possibility of modification of the code to fit demands laid on the numerical solution. The widely-used modern FVM schemes are based on TVD [47], ENO [35], Residual Distribution [36] and/or specific numerical flux computation (AUSM, HLLC... [39]) approach usually combined with Large-Eddy Simulation [34]. The unsteady effects are prevailingly modelled with the use of ALE [26] method (although for small changes of the reference frame the SDT can also be used). The recent knowledge on unsteady flows and aeroelasticity is summarised in [32].

Objectives of the Work

The main objectives of this work are to develop and implement various numerical methods for numerical solution of two and three-dimensional steady and unsteady inviscid transonic flow around an oscillating profile and a swept wing. This goal can be divided in following steps:

- Definition of mathematical model.
- Development and implementation of various modern high-order numerical schemes based on TVD approach in two dimensions.
- Implementation of suitable boundary condition in two dimensions.

- Implementation of unsteady effects (prescribed oscillations of the profile) using two different techniques: *Small Disturbance Theory* and *Arbitrary Lagrangian–Eulerian* Method.
- Extension of implemented 2D unsteady method into 3D.
- Numerical validation of both 2D and 3D methods with respect to numerical results of other authors and also to experimental data.

Achieved Results

In this work numerical results concerning two- and three-dimensional unsteady transonic inviscid flow are presented. In order to validate developed methods, numerical results are compared with results of other authors and experimental data for both steady and unsteady cases. Overall good agreement can be observed. Experimental results in the case of 3D unsteady flow were unfortunately not available to the author in the time of writing of this thesis. The results however look reasonable and in accordance with theory. Preliminary results of two-dimensional laminar viscous flow are also presented.

Acknowledgement

The author would like to thank to the supervisor Prof. RNDr. Karel Kozel DrSc. (Czech Technical University in Prague, Faculty of Mechanical Engineering), Prof. José Manuel Redondo (Universitat Politécnica de Catalunya, Departament de Física Aplicada) and Doc. Ing. Jiří Fürst, PhD. (CTU, Faculty of Mechanical Engineering). Great thanks belong also to the Aeronautical Research and Test Institute in Prague for providing the possibility of close cooperation.
This work has been partly supported by the Research plan of the Ministry of Education of the Czech Republic VZ MSM 6840770010 and project of the Grant Agency of the Czech Academy of Science of the Czech Republic GACR 201/08/0012.

1 Mathematical Models of Compressible Flows

Governing system of equations used for description of motion of viscous compressible fluids is presented by the Navier–Stokes equations [30]. The influ-

ence of viscous effects on the flow is however nearly negligible in some cases and hence a simpler model presented by the Euler equations can be chosen.

2 Navier–Stokes Equations

2.1 Navier–Stokes Equations

In the case of three-dimensional flow of viscous compressible fluid the Navier–Stokes Equation can be written in a following vector form:

$$\mathbf{W}_t + \mathbf{F}_x + \mathbf{G}_y + \mathbf{H}_z = 0, \tag{1}$$

where

$$\begin{aligned} \mathbf{F} &= \mathbf{F}^c - \mathbf{F}^v, \\ \mathbf{G} &= \mathbf{G}^c - \mathbf{G}^v, \\ \mathbf{H} &= \mathbf{H}^c - \mathbf{H}^v, \end{aligned}$$

and

$$\begin{aligned} \mathbf{W} &= \left(\rho, \rho u, \rho v, \rho w, e\right)^T, \\ \mathbf{F}^c &= \left(\rho u, \rho u^2 + p, \rho uv, \rho uw, (e+p)u\right)^T, \\ \mathbf{G}^c &= \left(\rho v, \rho uv, \rho v^2 + p, \rho vw, (e+p)v\right)^T, \\ \mathbf{H}^c &= \left(\rho w, \rho uv, \rho uw, \rho w^2 + p, (e+p)w\right)^T, \\ \mathbf{F}^v &= \left(0, \tau_{xx}, \tau_{xy}, \tau_{xz}, u\tau_{xx} + v\tau_{xy} + w\tau_{xz} + kT_x\right)^T, \\ \mathbf{G}^v &= \left(0, \tau_{xy}, \tau_{yy}, \tau_{yz}, u\tau_{xy} + v\tau_{yy} + w\tau_{yz} + kT_y\right)^T, \\ \mathbf{H}^v &= \left(0, \tau_{xz}, \tau_{yz}, \tau_{zz}, u\tau_{xz} + v\tau_{yz} + w\tau_{zz} + kT_z\right)^T. \\ \tau_{xx} &= \frac{2}{3}\eta(2u_x - v_y - w_z) \\ \tau_{yy} &= \frac{2}{3}\eta(-u_x + 2v_y - w_z) \\ \tau_{zz} &= \frac{2}{3}\eta(-u_x - v_y + 2w_z) \\ \tau_{xy} &= \eta(u_y + v_x) \\ \tau_{xz} &= \eta(u_z + w_y) \\ \tau_{yz} &= \eta(v_z + w_y) \\ \eta &= \eta(T) \end{aligned} \tag{2}$$

where $\mathbf{W}$ is vector of conservative variables, $\mathbf{F}^c, \mathbf{G}^c, \mathbf{H}^c$ are inviscid fluxes and $\mathbf{F}^v, \mathbf{G}^v, \mathbf{H}^v$ are viscous fluxes, ρ is density, (u, v, w) are velocity vector components, p is static pressure, e is total energy per unit volume, τ is tensor of viscous stresses, η is dynamical viscosity, T is temperature, Pr is the *Prandtl number* and k is heat transfer coefficient. Such a system contains the continuity equation (conservation of mass, first order, hyperbolic), the Navier-Stokes equation (conservation of momentum, second order, parabolic) and the conservation of energy equation (second order, parabolic). The whole system keeps the character of the individual equations, which in the case of Navier-Stokes equations is mixed parabolic-hyperbolic. System (1) is enclosed with the *Equation of state*:

$$p = (\kappa - 1)\big[e - \frac{1}{2}\rho(u^2 + v^2 + w^2)\big],\ \kappa = \frac{c_p}{c_v}. \tag{3}$$

Because

$$c_v T = \frac{\frac{p}{\rho}}{\kappa - 1} \quad \text{and} \quad k = \frac{\eta c_p}{Pr},$$

the heat flux in ideal gas may be computed using following relations

$$kT_x = \frac{\eta}{Pr}\frac{\kappa}{\kappa - 1}\Big(\frac{p}{\rho}\Big)_x, \quad kT_y = \frac{\eta}{Pr}\frac{\kappa}{\kappa - 1}\Big(\frac{p}{\rho}\Big)_y, \quad kT_z = \frac{\eta}{Pr}\frac{\kappa}{\kappa - 1}\Big(\frac{p}{\rho}\Big)_z. \tag{4}$$

Function $\eta(T)$ is then derived from Rayleigh relation

$$\frac{\eta(T)}{\eta(T_0)} = \Big(\frac{T}{T_0}\Big)^{\frac{3}{4}}$$

2.2 Euler Equations

2.2.1 3D Flow

If the viscous terms in (1) are neglected (i.e. $\boldsymbol{\eta} = 0$) the system of Euler equations describing flow of compressible inviscid fluid is obtained

$$\mathsf{W}_t + \mathsf{F}^c_x + \mathsf{G}^c_y + \mathsf{H}^c_z = 0. \tag{5}$$

Similarly like (1) also this system has to be enclosed with the Equation of state (3). The character of the system (5) is hyperbolic, because the terms with second derivatives on the right-hand side of equations (1), which express the influence of viscous effects, are neglected. From a certain point of view, the system of Navier-Stokes equations (1) may be understand as a parabolic perturbation of hyperbolic system of Euler equations (5).

3 Numerical Methods

3.1 Finite Volume Numerical Schemes

The numerical solution of considered flow problems was realised with the use of the following finite volume schemes in cell-centered form:

1. Lax–Wendroff scheme in Richtmyer form with additional artificial dissipation [24], [5],
2. Lax–Wendroff scheme in MacCormack form with additional artificial dissipation (special case are Causon's TVD and Modified Causon's schemes) [29], [47], [38]
3. Composite scheme [24], [5]

The additional artificial dissipation was chosen as

1. Mesh geometry dependent [5]
2. Jameson's artificial dissipation (various modifications [5], [24], [1])
3. Causon's TVD and Modified Causon's artificial dissipation [29], [38].

3.2 Numerical Methods for Unsteady flow

The unsteady flows were simulated using two different methods. The first one is a rather simple method based on Small Disturbations Theory (SDT), which can be used for simulation of oscillatory motion with one degree of freedom and under the assumption of small amplitudes. The second, more complex method, is called Arbitrary Lagrangian-Eulerian (ALE) method and is suitable for more difficult unsteady problems - considering more degrees of freedom and greater maximal amplitudes.

3.2.1 Small Disturbance Theory

Main idea of SDT is approximation of the rotation of an inviscid wall around a fixed point by the rotation of a normal vector to the wall, i.e. there is no real motion of the profile/wing and moreover the position of elastic axis is not taken into account. As mentioned above, this method is suitable only for motion with a small angle of rotation. In this work, SDT has been used for obtaining preliminary results of 3D unsteady flow around a swept wing

with NACA 0012 profile in order to investigate if proposed Modified Causon's scheme is able to handle also three-dimensional unsteady transonic flows. The maximal admissible used angle of attack in our computations was $\phi \leq 3°$. Let us consider the x axis of the coordinate system aligned with the chord of the profile with zero angle of attack. The AoA is considered positive in the case of clockwise rotation of the profile. The fluid velocity vector $(\mathsf{u}, \mathsf{v})^T$ on the profile surface has to satisfy the relation

$$\arctan\left(\frac{\mathsf{v}}{\mathsf{u}}\right) = \arctan(f') - \phi \tag{6}$$

where the graph of the function f defines either the lower or the upper side of the profile. This corresponds to the fact, that in the case of inviscid flow the profile surface is a streamline and hence the fluid velocity vector on the wall has to be tangent to the wall with normal vector $\mathbf{n}$. In SDT the vector $\mathbf{n}$ is rotated by the angle ϕ with respect to the normal vector $\mathbf{n}_w$ of the wall at a zero angle of rotation.

3.2.2 Arbitrary Lagrangian-Eulerian Method

Arbitrary Lagrangian Eulerian method combines the use of the classical Lagrangian and Eulerian reference frames, which are two basic reference frames in fluid dynamics. In the case of the Lagrangian reference frame the fluid motion is investigated by following individual fluid particles as they move through space and time. The Lagrangian reference frame is largely used most commonly in solid mechanics - it sets up a reference frame by fixing a grid to the material of interest and then as the material deforms the grid deforms with it. On the other hand in the case of the Eulerian reference frame a concrete area (points in space) through which the the fluid moves is observed. The Eulerian reference frame is the typical framework used in the analysis of fluid mechanics problems. It allows for material to flow through the grid. However, it does not track the path of any individual particle. The ALE approach allows for both a flexible grid and a grid that allows for material to flow through it. In essence, it takes the best part of both reference frames and combines them into one. This is helpful in problems with large deformations in solid mechanics and in fluid-structure interaction. The mentioned schemes have of course an other form in the case of unsteady computation with the ALE method than in the case of steady computation [25]. When using the ALE method in order to obtain numerical solution of unsteady flow on a moving and deforming grid one of the main demands laid on the method is

that it predicts a uniform flow because it is then mathematically consistent. This demand is satisfied only when the algorithm constructed for the mesh modifications and the numerical scheme chosen for numerical solution fulfil the discrete *Geometric Conservation Law* as shown in [25]. The Geometry Conservation Law states that the change in area of each cell between time t_n and t_{n+1} must be equal to the area swept by the cell boundary during $\triangle\mathsf{t} = \mathsf{t}_{n+1} - \mathsf{t}_n$.

3.2.3 Mathematical Prescription of the Airfoil and Wing motion

The unsteady effects considered in this work were given in both 2D and 3D cases by prescribed profile/wing oscillations around an elastic axis governed by the relation for pitching angle

$$\alpha_1(\mathsf{t}) = \phi_0 + \phi_1 \sin(\omega \mathsf{t}) \tag{7}$$

around the reference point x_{ref}, ϕ_0 is the initial deviation of the aerofoil and ϕ_1 is the maximal amplitude. The angular velocity is defined as

$$\omega = 2k\pi \frac{U_\infty}{c} \tag{8}$$

where U_∞ is the free-stream velocity, c is the chord length and k is the reduced frequency.

4 Numerical Results - Steady Flows

4.1 2D Flow

Two standard test cases are simulated using the schemes mentioned in 3 - 2D flow around the profile NACA 0012 and flow around DCA 18% in a channel.

4.1.1 Inviscid Flow past the NACA 0012 profile

Steady computation of flow around the NACA 0012 aerofoil was carried out using structured FVM mesh made from quadrilaterals with 8400 computational cells (140 cells around the profile). The solution domain covered by the computational mesh was 20 profile chords long and 20 profile chords wide. Flow was simulated in the following regimes

1. $M_\infty = 0.5$, AoA $= 0^\circ$ (AoA stands for angle of attack)

2. $M_\infty = 0.5$, AoA $= 1.25°$

3. $M_\infty = 0.8$, AoA $= 0°$

4. $M_\infty = 0.8$, AoA $= 1.25°$

For the numerical simulation the following FVM schemes were chosen

1. Modified Causon's scheme (i.e. LW MacCormack with modified Causon's artificial dissipation)

2. LW Richtmyer scheme with Jameson's artificial dissipation

3. Composite scheme (i.e. LW Richtmyer + LF)

Figures 1, 2 show inviscid numerical results achieved by LW scheme in Richtmyer and MacCormack form and by the Composite scheme. The results are shown in the form of Mach number and c_p isolines for $M_\infty = 0.8$ and both zero and non-zero inlet angles of attack. The distribution of Mach number and c_p along top and bottom side of the profile for subsonic as well as transonic flow is also compared. It is obvious that proposed (and implemented) schemes are in a good correspondence with the results of other authors and also with the expectation about the behaviour of investigated flow regimes.

4.1.2 Viscous Laminar past the NACA 0012 profile

The viscous laminar flow simulation was realised with the use of Modified Causon's scheme for Reynolds numbers $Re = 10^4$ and $Re = 10^5$, $M_\infty = 0.5$, 0.8 and AoA $= 0°$. In the case of the lower velocity, i.e. for inlet Mach number $M_\infty = 0.5$, the scheme performed as expected - laminar boundary layer tightens with increasing Reynolds number. However, in the case of inlet Much number $M_\infty = 0.8$ the flow becomes unsteady even for $Re = 10^4$ (see unsteady behaviour of the solution in the wake Fig. 3). Such a fact can not be unfortunately verified as there are no experimental data available for flow characterised by this values of inlet velocity and Reynolds number.

4.1.3 Flow past the DCA 18% profile in a channel

In the case of inviscid flow over the DCA 18% profile the MacCormack scheme combined with Jameson's artificial dissipation was used. The results for both subsonic and transonic flow were compared with experimental data from Institute of Thermomechanics, Czech Academy of Science. As can be seen

in figure 4 there is a good correspondence between the experimental and numerical results in the case of subsonic flow. On the other hand, the results for transonic flow differ. This is caused above all by the fact that the chosen mathematical model was considered inviscid while the experiment was carried out under the condition of $Re = 5 \cdot 10^6$. Moreover, from the experimental results is clear that the real flow field became unsteady.

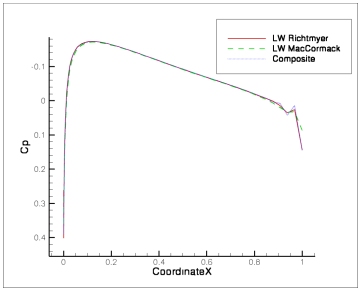

$M_\infty = 0.5$, angle of attack $\alpha_1 = 0°$

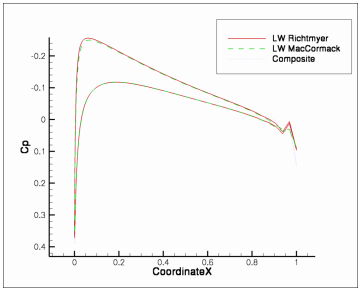

$M_\infty = 0.5$, angle of attack $\alpha_1 = 1.25°$

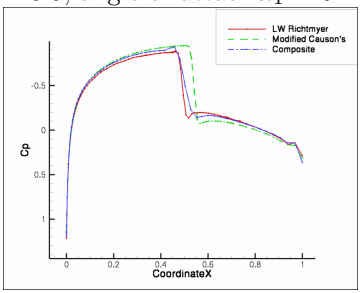

$M_\infty = 0.8$, angle of attack $\alpha_1 = 0°$

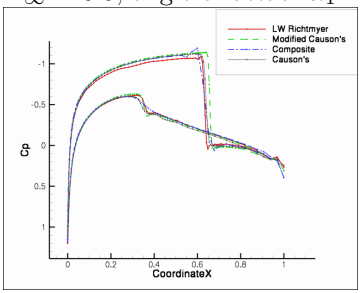

$M_\infty = 0.8$, angle of attack $\alpha_1 = 1.25°$

Figure 1: NACA 0012, c_p distribution alongside the profile, comparison of used schemes.

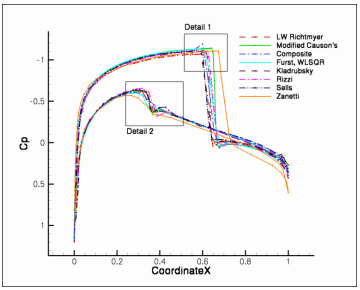

(a) c_p distribution alongside the top and bottom side of the aerofoil

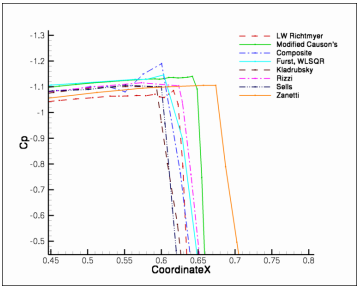

(b) Detail 1, c_p distribution on the top-side shock wave.

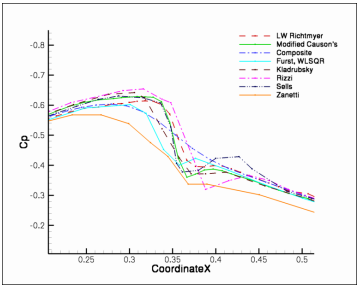

(c) Detail 2, c_p distribution on the bottom-side shock wave.

Figure 2: NACA 0012, $M_\infty = 0.8$, angle of attack $\alpha_1 = 1.25°$, c_p distribution on the profile, comparison of used schemes and schemes from other authors.

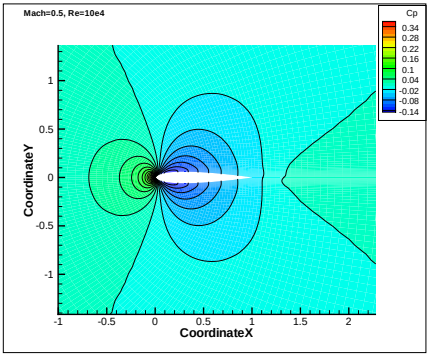

c_p, $M_\infty = 0.5$, $Re = 10^4$

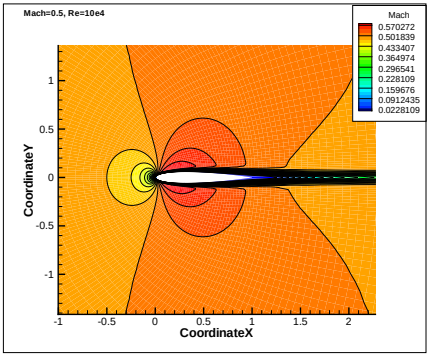

Mach Number, $M_\infty = 0.5$, $Re = 10^4$

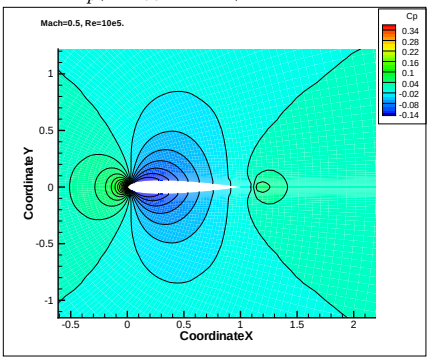

$c_p, M_\infty = 0.5$, $Re = 10^5$

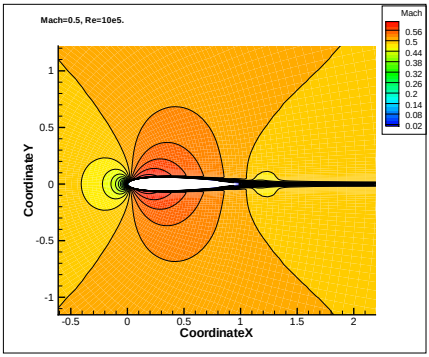

Mach number, $M_\infty = 0.5$, $Re = 10^5$

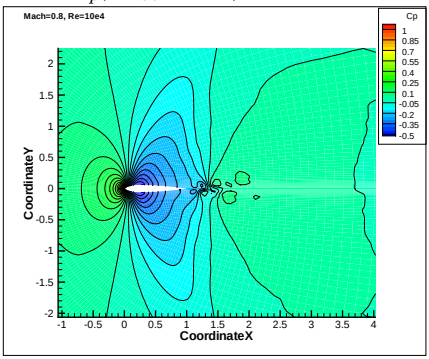

c_p, $M_\infty = 0.8$, $Re = 10^4$

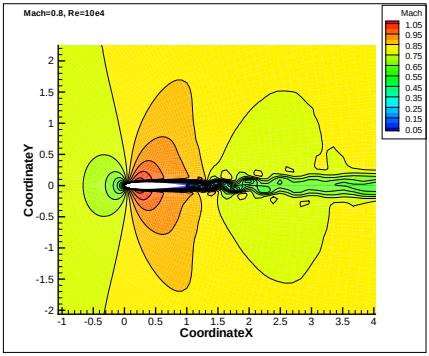

Mach number, $M_\infty = 0.8$, $Re = 10^4$

Figure 3: NACA 0012, viscous laminar flow, $M_\infty = 0.5, 0.8$, angle of attack $\alpha_1 = 0°$, c_p and Mach number distribution.

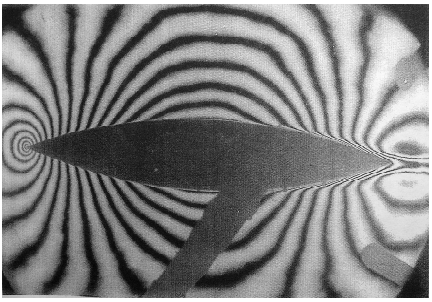

Experimental results, $M_\infty = 0.526$

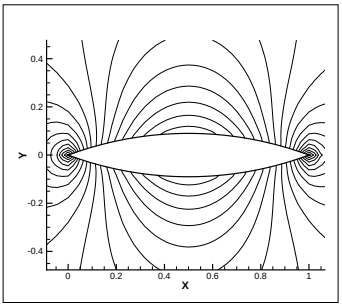

Numerical results, $M_\infty = 0.526$

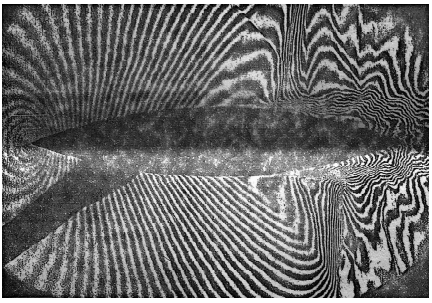

Experimental results, $M_\infty = 0.79$

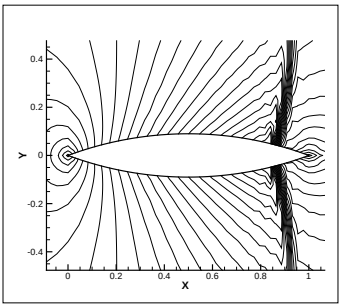

Numerical results, $M_\infty = 0.79$

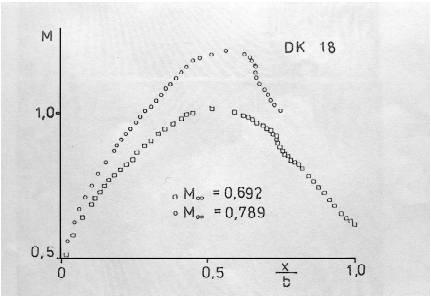

Experimental results.

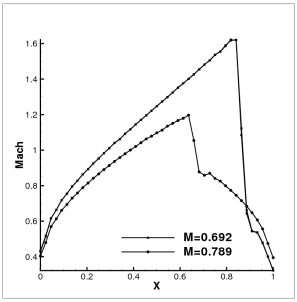

Numerical results

Figure 4: DCA 18% in a channel, comparison of experimental and numerical results, Mach number isolines [a) - d)] and its behaviour on the profile.

4.2 3D Flow

Two different cases were chosen for the simulation of three-dimensional flow. At first a simple geometry of a fictitious swept wing with NACA 0012 profile fixed in a wall has been used and two flow regimes based on the known two-dimensional test cases were simulated to obtain preliminary results of 3D computation. Then the standard 3D test case - the transonic flow over the ONERA M6 wing was successfully simulated and compared with the results of other authors and experimental data.

4.2.1 Flow over the NACA 0012 swept wing

The flow regimes were characterised by the following inlet Mach number and the angle of attack

1. $M_\infty = 0.8$, angle of attack $\alpha_1 = 0°$
2. $M_\infty = 0.8$, angle of attack $\alpha_2 = 1.25°$

The wing has the NACA 0012 profile and spread of 3 profile chords. The tip-chord equals one-half of the root-chord. Numerical results can be seen on Fig. 5 . As there are no experimental data available for this case of flow, the only usable reference present the 2D results for the same initial condition (Fig. 1, 2). The 3D results obtained on H-type structured mesh with 253715 elements show all the important characteristic that can be expected according to the knowledge of the 2D results.

4.2.2 Flow over the ONERA M6 wing

The 3D inviscid transonic flow over the ONERA M6 wing was characterised by the inlet Mach number $M_\infty = 0.8395$ and the angle of attack $\alpha_1 = 3.06°$. For the computation two modification of LW scheme were chosen (later denoted as Method 1 and Method 5). Numerical results obtained by the author were compared to the results of other authors (Methods 2 - 4) and to the experimental data [46] with a very good agreement (Fig. 6 - 7).

Method 1 As the first method the cell-centred 3D MacCormack predictor-corrector scheme with 3^{rd} order Jameson's artificial dissipation was chosen. Although this scheme does not posses the TVD property, for properly chosen coefficients it is able to deliver results comparable with TVD

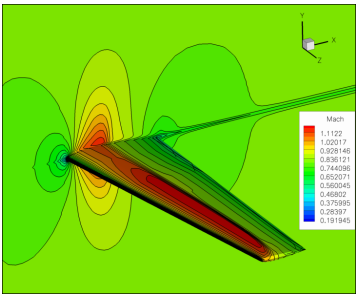

a) c_p coefficient, angle of attack $\alpha_1 = 0°$

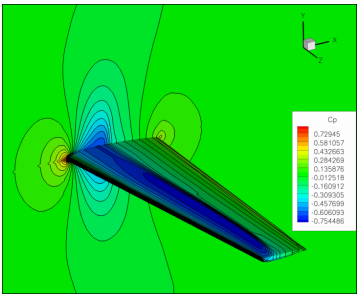

b) Mach number, angle of attack $\alpha_1 = 0°$

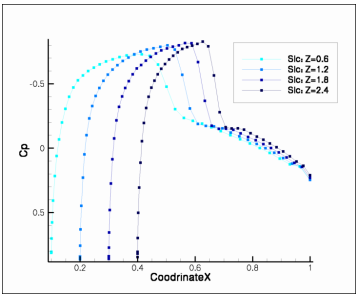

c) c_p coefficient in the cuts, AoA $\alpha_1 = 0°$

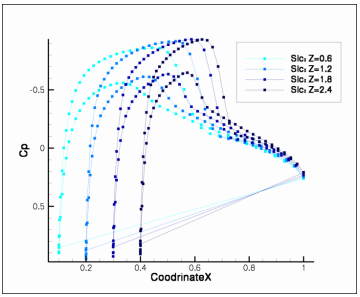

d) c_p coefficient in the cuts, AoA $\alpha_2 = 1.25°$

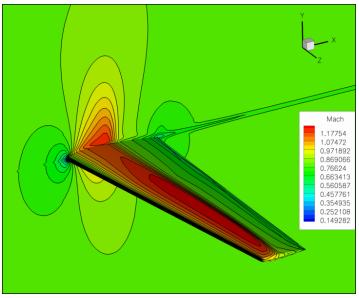

e) c_p coefficient, angle of attack $\alpha_2 = 1.25°$

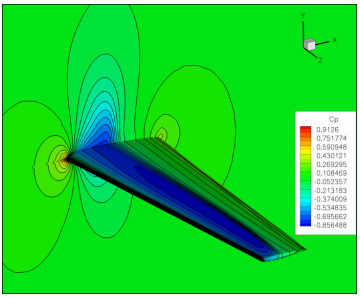

f) Mach number, angle of attack $\alpha_2 = 1.25°$

Figure 5: NACA 0012 swept wing, $M_\infty = 0.8$, angle of attack $\alpha_1 = 0°$, $\alpha_2 = 1.25°$. Distribution of the c_p coefficient and Mach number on the top side of the wing and in the cuts 20%, 40%, 60% and 80% of the wing spread.

variant of MacCormack scheme. For the discretisation of the computational area following FVM meshes were used: C-mesh with 493000 cells and H-mesh with 687456 cells. The code was parallellised with the use of the OpenMP library. Method was implemented by the author.

Method 2 In this case the cell-vertex Ron-Ho-Ni scheme described in [1], [40] was used. It is one-step explicit Lax–Wendroff-type scheme with 3^{rd} order Jameson's artificial dissipation. The same computational C-type mesh as for Method 1 was used. Method was implemented by Milan Kladrubský (VZLU a.s.).

Method 3 The computational area was discretised by an unstructured mesh with quadrilateral computational cells. The problem was solved by FVM in a cell-centred formulation - the Roe-Riemann solver [41] was used to solve the Riemann problem on each side of each finite volume. Spatial accuracy of the method was increased by linear reconstruction using the Least Square method [42]. For the time discretisation the linearised backwards Euler method was used. Final system of equation was solved by GMRES method with ILU preconditioning. Method was implemented by Jiří Dobeš (CTU, Faculty of Mechanical Engineering).

Method 4 This method is an extension of the high-order FVM weighted least-square (WLSQR) scheme mentioned in [28] into three dimensions. The high order WLSQR reconstruction is combined with the HLLC numerical flux and the resulting semi-discrete system of equations is solved by the linearised backward Euler method. Resulting sparse system of linear equations is then solved with GMRES method [33] with modified ILU(0) preconditioner. Computational mesh was the same as in Method 3. Method was implemented by Jiří Fürst (CTU, Faculty of Mechanical Engineering).

Method 5 Modified Causon's scheme in 3D form. Computation was carried out using the same C-type mesh as in Method 1. The code was parallellised with the use of the OpenMP library. Method was implemented by the author.

Comparison between numerical and experimental results in the case of 3D flow shows that both schemes implemented by the author give very similar results. The correspondence with experimental data is satisfactory. Both the position and intensity of shock waves are captured reasonably well. The

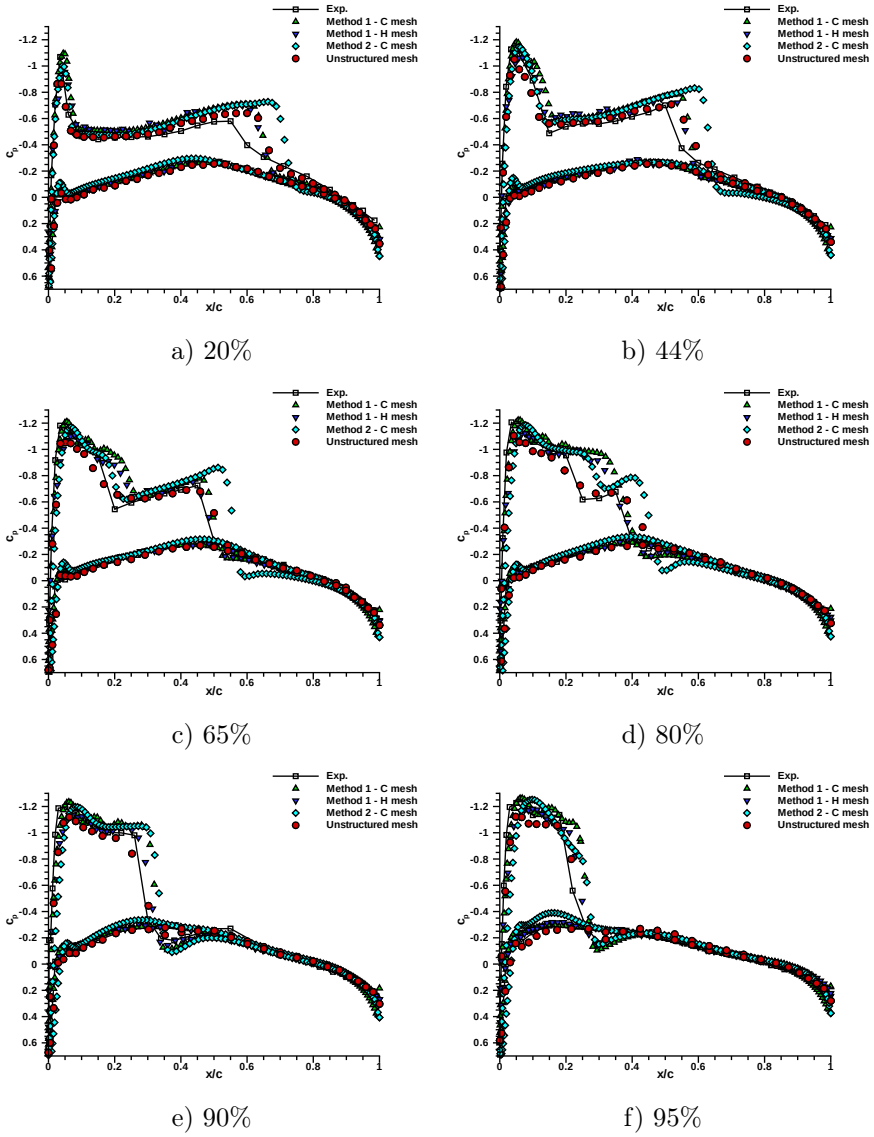

Figure 6: ONERA M6, $M_\infty = 0.8395$, angle of attack $\alpha_1 = 3.06°$. Methods 1, 2 and 3. Comparison with the experimental results [46]. Distribution of the c_p coefficient in the cuts alongside the wing.

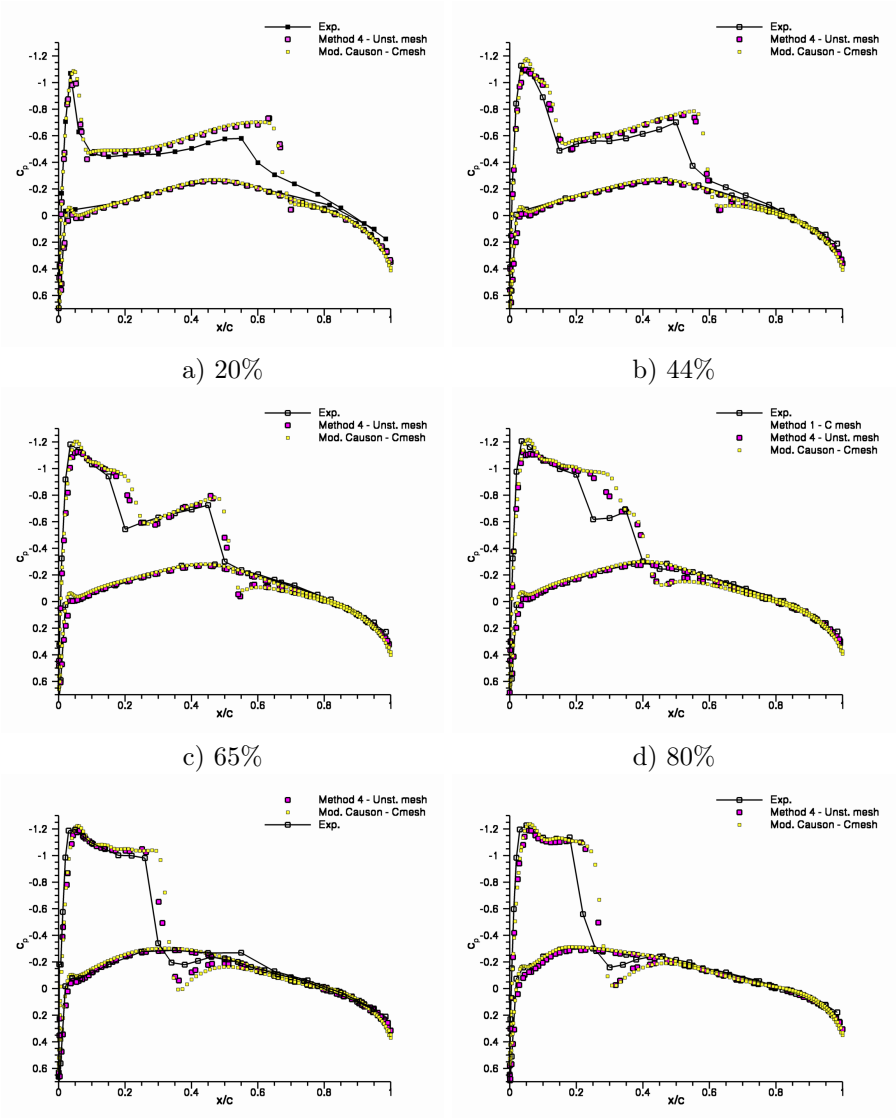

a) 20% b) 44%

c) 65% d) 80%

e) 90% f) 95%

Figure 7: ONERA M6, $M_\infty = 0.8395$, angle of attack $\alpha_1 = 3.06°$. Methods 4 and 5. Comparison with the experimental results [46]. Distribution of the c_p coefficient in the cuts alongside the wing.

observed differences are highly probable consequence of inviscid nature of the chosen model, which collide with viscous turbulent behaviour of the real flow. The Modified Causon's scheme (as well as the LW MacCormack scheme with Jameson's artificial dissipation) has somewhat limited use because of its explicit form and its ability to handle only the structured meshes. The first drawback can be removed by using the implicit version of the scheme [47]. Its demands on the computational time are however comparable with the WLSQR scheme and Roe-Riemann solver, but it needs much less memory. WLSQR scheme and the Roe-Riemann solver are on the other hand able to solve greater variety of problems described also by unstructured meshes.

5 Numerical Results - Unsteady Flows

5.1 2D Flow

5.1.1 Flow past the DCA 18% profile

Functionality of the LW MacCormack scheme with Jameson's AD in the combination with ALE method was tested on the case of inviscid subsonic flow over the DCA 18% aerofoil in a channel. The oscillatory motion of the profile around the reference point $\mathsf{x}_{ref} = [\frac{1}{3}, 0.00]$ is given by (7) with initial deviation $\phi_0 = 0°$ and maximal amplitude $\phi_1 = 1.25°$. The angular velocity is defined as

$$\omega = 2k\pi \frac{U_\infty}{c} \tag{9}$$

where U_∞ is the free-stream velocity, c is the chord length and the reduced frequency is $k = 0.08$ and $M_\infty = 0.755$. The unsteady state development is observed on the lift coefficient (c_n) behaviour, where

$$c_n = \frac{\oint P dx}{\frac{1}{2} u_{ref}^2 \rho_{ref}} \tag{10}$$

As can be seen from the figure 8 the flow becomes periodic after one period of unsteady computation and the numerical solution possess all the characteristics as expected.

5.1.2 Flow past the NACA 0012 profile

Considered test case is a transonic flow over an oscillating NACA 0012 profile for which the experimental data are available in [45]. The oscillatory motion is governed by the equation (7) and is characterised by

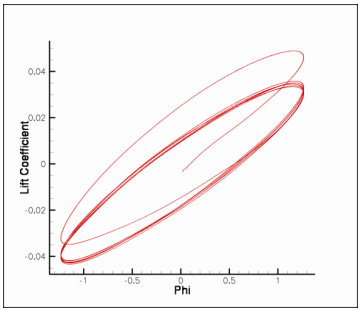

Figure 8: DCA 18%, lift coefficient behaviour during the unsteady computation, LW MacCormack scheme with Jameson's artificial dissipation.

- the inlet Mach number $M_\infty = 0.755$
- the reference point $\mathsf{x}_{ref} = [0.25, 0.00]$
- the initial deviation of the profile $\phi_0 = 0.016°$
- the maximal amplitude $\phi_1 = 2.51°$
- and the reduced frequency $k = 0.0814$ (in (9))

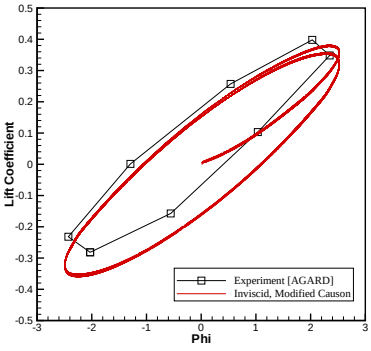

(a) Modified Causon's scheme.

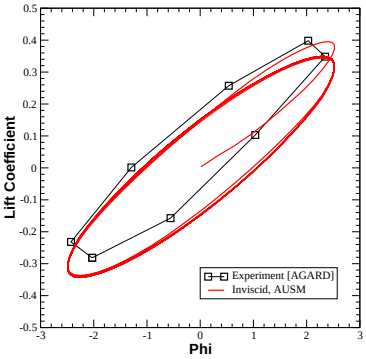

(b) WLSQR scheme with AUSMPW+ flux.

Figure 9: NACA 0012, lift coefficient behaviour.

Computation was carried out using Modified Causon's scheme and same structured C-type mesh as in section 4.1.1. The results were compared with results obtained by J. Fürst using the WLSQR scheme with AUSMPW+ flux [28] on unstructured mesh with 6720 quadrilateral cells (120 cells around profile). As can be seen from the figures 9 - 10 the Modified Causon's scheme performs well. The results correspond qualitatively, but the experimental data show a bit higher c_n values (Fig. 9). Considering the symmetry of simulated problem, also the behaviour of the c_n should be symmetric with the center of symmetry in point $[0, 0]$. The experimental data however do not posses this characteristic and therefore a suspicion of their systematical error comes in mind. Important characteristics, as for example the position and strength of the shock wave, are however in a good correspondence.

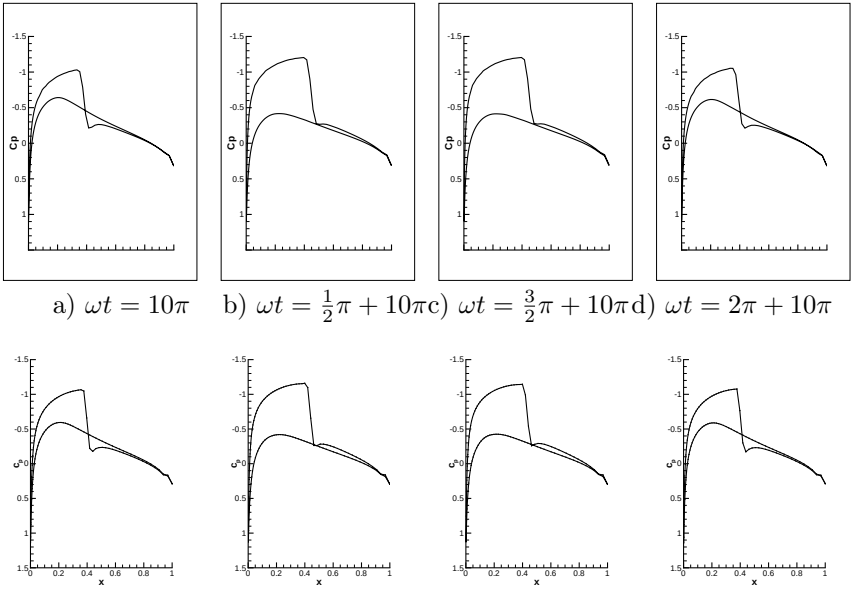

a) $\omega t = 10\pi$ b) $\omega t = \frac{1}{2}\pi + 10\pi$ c) $\omega t = \frac{3}{2}\pi + 10\pi$ d) $\omega t = 2\pi + 10\pi$

e) $\omega t = 10\pi$ f) $\omega t = \frac{1}{2}\pi + 10\pi$ g) $\omega t = \frac{3}{2}\pi + 10\pi$ h) $\omega t = 2\pi + 10\pi$

Figure 10: c_p behaviour during 5^{th} period of the oscillatory motion, Modified Causon's Scheme (a-d) WLSQR scheme with AUSMPW+ flux (e-h).

5.2 3D Flow

5.2.1 Flow over the NACA 0012 swept wing

A fictitious swept wing same as in the section 4.2.1 was used for the first test of the LW MacCormack scheme with Jameson's artificial dissipation in combination with Small Disturbance Theory. The flow was characterised by

- The inlet Mach number $M_\infty = 0.8$,
- Forced oscillatory motion around an elastic axis parallel with the axis z was again given by (7)

$$\alpha_1(\mathsf{t}) = \phi_0 + \phi_1 \sin(\omega \mathsf{t}), \quad \omega = 2f\pi$$

  with
  - initial deviation $\phi_0 = 1°$,
  - maximal amplitude $\phi_1 = 0.25°$
  - frequency $f = 10\text{Hz}$

Obtained numerical results show that the fully periodical state of the flow was achieved during the third period of the computation. Although the results are satisfactory, the SDT is however not the ideal way to simulate such a complicated problem as 3D unsteady flow because it does not concern the reference point through which leads the elastic axis and therefore neglects an important flow characteristic.

5.2.2 Flow over the ONERA M6 wing

More complex 3D computation was carried out using the ALE method. The initial conditions were taken from the steady result (section 4.2.2). The forced oscillatory motion of the wing around the elastic axis parallel with the axis z and going through the reference point $\mathsf{x}_{ref} = [\frac{1}{2}; 0.00; 0.00]$ was given by the same relation for pitching angle as in 2D (7). The inlet Mach number was considered $M_\infty = 0.8395$, initial deviation $\alpha_0 = 3.06°$, amplitude $\alpha_1 = 1.5°$. The computational mesh was the same structured C-type mesh as in Sec. 4.2.2. The Modified Causon's scheme has proved itself well - the results (Fig. 12) show that the fully periodic state has been achieved at least during the 3^{rd} period of the oscillatory motion. Both shock waves on the top side of the profile, which are characteristic for this type of flow over the ONERA M6 wing, move on the wing surface throughout the period as expected and

the scheme does not produce spurious oscillations. Comparison with the experimental data is unfortunately not yet available, but at the present time a work is in progress on implementation of another wing geometry used in the experiments with oscillating wing at the Aeronautical Research and Test Institute in Prague.

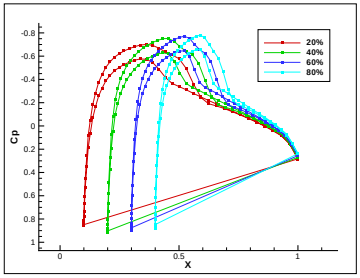

a) Steady result.

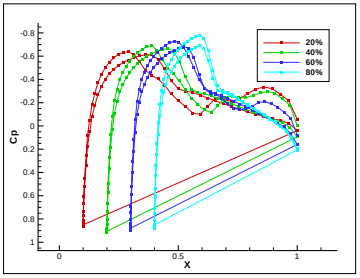

b) Non-steady result, $\omega t = 6\pi$.

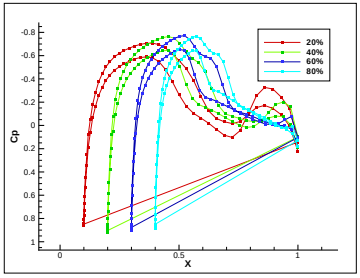

c) Non-steady result, $\omega t = \frac{1}{2}\pi + 6\pi$.

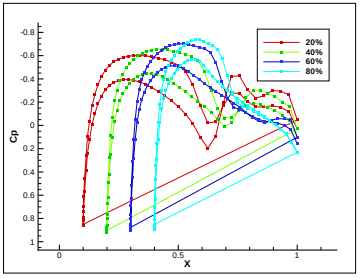

d) Non-steady result, $\omega t = \pi + 6\pi$.

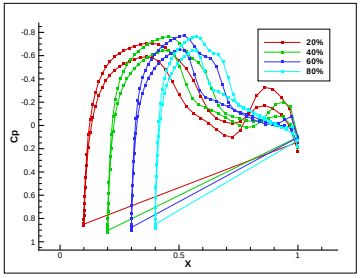

c) Non-steady result, $\omega t = \frac{3}{2}\pi + 6\pi$.

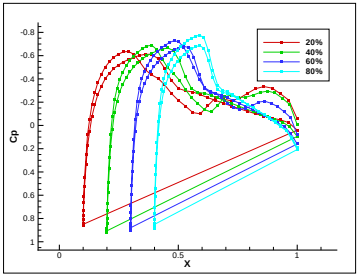

d) Non-steady result, $\omega t = 2\pi + 6\pi$.

Figure 11: NACA 0012 wing, c_p coefficient behaviour during 3^{rd} period of forced oscillatory motion. $M_\infty = 0.8, \phi_0 = 1°, f = 10\,\text{Hz}, \phi_1 = 0.25°$, cuts alongside the wing in $20\%, 40\%, 60\%, 80\%$ of the wing spread.

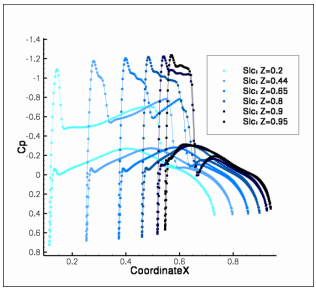

a) Steady result.

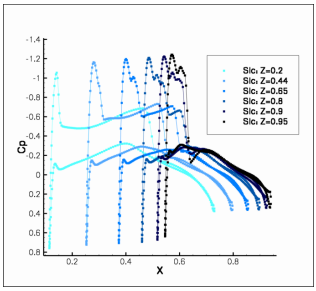

b) Non-steady result, $\omega t = 0\pi + 3\pi$.

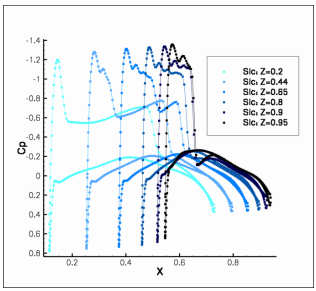

c) Non-steady result, $\omega t = \frac{1}{2}\pi + 3\pi$.

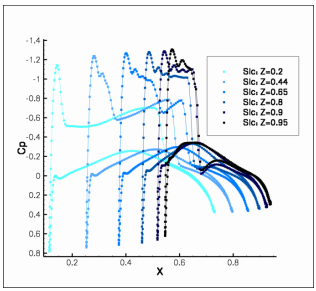

d) Non-steady result, $\omega t = \pi + 3\pi$.

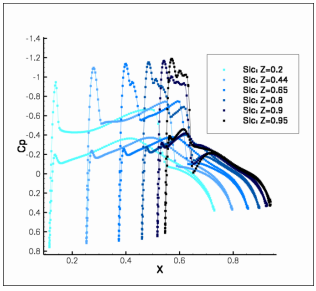

c) Non-steady result, $\omega t = \frac{3}{2}\pi + 3\pi$.

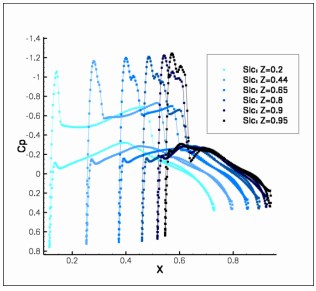

d) Non-steady result, $\omega t = 2\pi + 3\pi$.

Figure 12: ONERA M6 wing, c_p coefficient distribution in the cuts alongside the wing during 3^{rd} period of the oscillatory motion. $M_\infty = 0.8395, k = 10\,\text{Hz}, \phi_1 = 1.5°$

6 Conclusion

The objectives of the thesis have been fullfiled. The mathematical background for numerical solution of hyperbolic equations is presented also with a simple analysis of boundary and initial conditions. The way of TVD schemes construction is described and the basic properties of FVM schemes based on Lax–Wendroff approach are investigated in the case of 1D scalar initial value problem. Three different FVM methods with five types of artificial dissipation are introduced for both 2D and 3D and used for the numerical simulations of subsonic and transonic inviscid flow (one of the methods is extended also for viscous laminar flows). 3D numerical results of transonic inviscid flow over the ONERA M6 wing is compared with the results of other authors as well as with the experimental data with a very good agreement (the best results have been obtained with the so called Modified Causon's scheme). Two different approaches to the numerical solution of unsteady flow considering forced oscillation of a profile and a wing are applied. Firstly a simple Small Disturbance Theory model is used for the simulation of 3D inviscid transonic flow around a fictitious swept wing. Obtained results show that fully periodic state is achieved. Then a more advanced way using the Arbitrary Lagrangian-Eulerian method is proposed and implemented. The results of 2D unsteady flow are compared with experimental data obtained by NASA and numerical results by J. Fürst. A good agreement can be observed. The 3D extension of implemented method is used for solution of transonic inviscid flow over the ONERA M6 wing with satisfactory results (the comparison to experimental data is unfortunately not yet available). According to this facts, the proposed method is proved as a reliable numerical simulation of chosen flow regimes and is expected to be able to solve also other problems of similar nature. For broader use the method would however need a deeper numerical validations.

The presented results are in a form of distribution of Mach number and c_p coefficients (both 2D and 3D) which are completed by the behaviour of the lift coefficient in the case of unsteady flow.

The future steps intended are extension of 3D unsteady inviscid method also for the case of turbulent flow and introduction of one more degree of freedom, i.e. implementation of aeroelastic effects.

References

Author's Published and Unpublished Works

Published Works

[1] Dobeš, J., Fořt, J., Fürst J., Furmánek P., Kladrubský, M., Kozel, K., Louda, P. *Numerical Solution of Transonical Flow around a Profile and a Wing II.* Research report V-1850/05, VZLU a.s. 2005

[2] Dobeš, J., Fořt, J., Furmánek, P. , Fürst, J., Kladrubský, M., Kozel, K. *Numerical Solution of Transonical Flow around a Profile and a Wing III.* Research report R–4008, VZLU a.s., 2006

[3] Dobeš, J., Furmánek, P., Fořt, J., Fürst, J., Holman, J., Kladrubský, K., Kozel K. *Numerical Solution of Transonical Flow around a Profile and a Wing IV.* Research report R-4182, VZLU a.s. 2007

[4] Furmánek, P., Fürst, J., Kozel, K. *Numerical Solution of Nonsteady Flow around a Wing* Research report R-4428, VZLU a.s. 2007

[5] Furmánek, P. Numerical Solution of Transonic Flow over an Isolated Profile, Diploma thesis (in Czech), ČVUT FJFI, Praha, 2004.

[6] Furmánek, P. , Fürst, J., Kozel, K. Numerical Simulation of Unsteady Flow in 2D and 3D In: Topical Problems of Fluid Mechanics 2009. Praha: Ústav termomechaniky AV ČR, 2008, p. 33-36. ISBN 978-80-87012-12-9.

[7] Furmánek, P., Fürst, J., Kozel, K. Numerické řešení 3D stacionárního a nestacionárního obtékání křídla In: Transfer - Výzkum a vývoj pro letecký průmysl [online]. 2008, roč. 3, č. 8, s. 72-77.ISSN 1801-9315. Internet: www.vzlu.cz/content.php?ctg=2

[8] Furmánek, P., Fořt, J., Kladrubský, M., Kozel, K. Numerical Simulation of Steady and Unsteady 3D Flow over a Swept Wing In: Topical Problems of Fluid Mechanics 2008. Praha: Ústav termomechaniky AV ČR, 2008, p. 39-42. ISBN 978-80-87012-09-3.

[9] Furmánek, P., Dobeš, J., Fürst, J., Kladrubský, M., Kozel, K. Numerické řešení některých problémů vnější a vnitřní aerodynamiky In: Transfer - Výzkum a vývoj pro letecký průmysl [online]. 2007, roč. 2, č. 4, s. 72-77.ISSN 1801-9315. Internet: www.vzlu.cz/content.php?ctg=2

[10] Dobeš, J., Fořt, J., Furmánek, P., Fürst, J., Kladrubský, M., et al. Numerical Solution of a Transonic Turbulent Flows over an Airfoil In: Topical Problems of Fluid Mechanics 2007. Praha: Ústav termomechaniky AV ČR, 2007, p. 33-36. ISBN 978-80-87012-04-8.

[11] Furmánek, P., Fürst, J., Kozel, K., Dobeš, J., Fořt, J., et al. Numerical Solution of Steady and Unsteady Transonic Flow over a Profile and a Wing In: Topical Problems of Fluid Mechanics 2007. Praha: Ústav termomechaniky AV ČR, 2007, p. 45-48. ISBN 978-80-87012-04-8.

[12] Furmánek, P., Horáček, J., Kozel, K. Numerical Solution of Steady and Unsteady Flow over a Profile in a Channel In: Colloquium Fluid Dynamics 2007 [CD-ROM]. Praha: Ústav termomechaniky AV ČR, 2007, ISBN 978-80-87012-07-9.

[13] obeš, J., Fořt, J., Furmánek, P., Fürst, J., Kladrubský, M., et al. Numerické řešení stacionárního a nestacionárního transsonického proudění ve vnější aerodynamice In: Colloquium Fluid Dynamics 2007 [CD-ROM]. Praha: Ústav termomechaniky AV ČR, 2007, ISBN 978-80-87012-07-9.

[14] Furmánek, P., Fürst, J., Horáček, J., Kozel, K. Numerical Solution of Some Problems of External and Internal Aerodynamics In: Topical Problem of Fluid Mechanics 2006. Praha: Ústav termomechaniky AV ČR, 2006, p. 55-58. ISBN 80-85918-98-6.

[15] Furmánek, P., Fürst, J., Horáček, J., Kozel, K. Numerical Solution of Transonic Flow over a Profile and around a Wing In: Application of Experimental and Numerical Methods in Fluid Mechanics. čilina: University of Žilina, Mechanical Engineering Faculty, 2006, p. 171-176. ISBN 80-8070-533-X.

[16] Furmánek, P., Dobeš, J., Fořt, J., Fürst, J., Kladrubský, M., et al. Numerical Solution of Transonic Flows over an Airfoil and a Wing In: CMFF'06 Conference Proceedings [CD-ROM]. Budapest: Budapest University of Technology and Economics, Department of Fluid Mechanics , 2006, p. 249-255. ISBN 963- 420-872-X.

[17] Furmánek, P., Fürst, J., Horáček, J., Kozel, K. Numerické řešení transsonického obtékání profilu a křídla In: Transfer - Výzkum a vývoj pro letecký průmysl [online]. 2006, roč. 1, č. 2, s. 103-109. Internet: www.vzlu.cz/content.php?ctg=2. ISSN 1801-9315.

[18] Furmánek, P., Fürst, J., Kozel, K., Mastný, P. Numerical Solution of Transonic Flow over an Airfoil In: Colloquium FLUID DYNAMICS 2005. Praha: Ústav termomechaniky AV ČR, 2005, p. 41- 44. ISBN 80-85918-94-3.

[19] Furmánek, P., Fürst, J., Kozel, K. Numerical Solution of Subsonic and Transonic Flow over a Profile Numerical Simulation of Complex and Multiphase Flows, IGESA Porquerolles, 2005, pččspčvek na konferenci.

[20] Mastný, P., Furmánek, P., Fürst, J., Kozel, K. Numerical Solution of 2D Inviscid Transonic Flow Past a Profile In: Topical Problems of Fluid Mechanics 2005. Praha: Ústav termomechaniky AV ČR, 2005, p. 69-72. ISBN 80-85918-92-7.

[21] Furmánek, P., Fürst, J., Kozel, K. Numerical Solution of Inviscid Transonic Flow over Profile In: Topical Problems in Fluid Mechanics 2004. Praha: Ústav termomechaniky AV ČR, 2004, p. 53-54. ISBN 80-85918-86-2.

Works Prepared for Publication

[22] Furmánek, P., Fürst, J., Kozel, K. High Orger Finite Volume Schemes for Numerical Solution of 2D and 3D Transonic Flows In: Kyberetika, International journal published by Institute of Information Theory and Automation, ISSN 0023-5954 ,

[23] obeš, J., Fořt, J., Furmánek, P., Fürst, J., Kladrubský, M., Kozel, K. Numerical Simulation of 3D Transonic Inviscid Flow over a Swept Wing In: Proceedings of the Czech–Japanese Seminar in Applied Mathematics 2008, University of Miyazaki, Miyazaki, Japan, September 4-7, 2008

Bibliography

[24] Kozel, K., Dvořák, Matematické modelování v aerodynamice (in Czech), 1st Edition, Vydavatelství ČVUT, Praha, 1996.

[25] Lesoinne, M., Farhat, C., Geometric conservation laws for flow problems with moving boundaries and deformable meshes, and their impact on aeroelastic computations, Computer Methods in Applied Mechanics and Engineering 134 (1996) 71-90.

[26] Feistauer, M., Felcman, J., Straškraba, I., Mathematical and Computational Methods for Compressible Flow. Oxford University Press, 2003. ISBN0 0 19 850588 4.

[27] Le Veque, R. J., Numerical Methods for Conservation Laws. Birkhäuser Verlag, Basel, 1990.

[28] Fürst J., A weighted least square scheme for compressible flows. *Flow, Turbulence and Combustion*, 76(4):331–342, June 2006.

[29] Fürst J., Numerical modeling of the transonic flows using TVD and ENO schemes. PhD thesis, ČVUT v Praze and l'Université de la Méditerranée, Marseille, 2001.

[30] Fürst J., Numerical Solution of Compressible Flows Using TVD and ENO Finite Volume Methods, Habilitation thesis, ČVUT, Praha, 2004.

[31] Honzátko, R., Numerical Simulations of Incompressible Flows with Dynamical and Aeroelastic Effects., Dissertation thesis, ČVUT, Praha, 2007

[32] Dowell, E. H., Clark, R., Cox, D., Curtiss, H. C. Jr., Edwards, J. W., Hall, K. C., Peters, D. A., Scanlan, R., Simiu, E., Sisto, F., Strganac, T. W. A Modern Course in Aeroelasticity, 4th Edition, Kluwer Academic Publishers, 2004.

[33] Saad, Y. and Schultz, M. *GMRES: A Generalized Minimal Residual Algorithm for Solving Nonsymmetric Linear Systems.* SIAM J. Sci. Statist. Comput. 7, 856-869, 1986.

[34] Lesieur M., Olivier M., Comte P., Large-Eddy Simulation of Turbulence Cambridge University Press, ISBN-13 978-0-521-78124-4, 2005,

[35] Harten, A., Enquist, B., Osher, S., Chakravarthy, S. Uniformly high order essentially non-oscillatory schemes iii. Journal of Computational Physics, 71:231-303, 1987.

[36] Abgrall, R., Barth, T., Residual distribution schemes for conservation laws via adaptive quadrature. SIAM J. Sci. Comput., 24(3):732-769, 2002. 3, 18

[37] Jameson, A., Schmidt, W., Turkel, E., Numerical solution of the Euler equations by fnite volume methods using Runge-Kutta time-stepping schemes, in: AIAA Paper 1981-1259, Palo Alto, California, 1981.

[38] Causon, D. M., High resolution fnite volume schemes and computational aerodynamics. In Josef Ballmann and Rolf Jeltsch, editors, Nonlinear Hyperbolic Equations - Theory, Computation Methods and Applications, volume 24 of Notes on Numerical Fluid Mechanics, pages 63-74, Braunschweig, March 1989. Vieweg.

[39] Liou, M., S., Steffen, J., Ch., A New Flux Splitting Scheme *Journal of Computational Physics* 107: 23–39, 1993

[40] Pelant J., Kyncl M., Kladrubský M. *Project of CFD methods for the three-dimensional inviscid compressible flow around wings and cascades.* Zpráva VZLÚ, V-1817/04, 2004

[41] Roe, P. L. *Approximate Riemann Solvers, Parameter Vector and Difference Schemes.* J. Comput. Phys. vol 43, pp 357 - 372. 1981.

[42] Barth T. J. and Jesperson D. C. *The Design of Upwind Schemes on Unstructured Meshes.* AIAA Paper 89–0366. 1989.

[43] Batten, P., Leschziner, M. A., Goldberg, U. C.: Average-State Jacobians and Implicit Methods for Compressible Viscous and Turbulent Flows, Journal of computational physics 137, 1997

[44] Cook, P. H., McDonald, M. A., Firmin, M. C. P.: Aerofoil RAE 2822 - pressure distributions and boundary layer and wake measurements, AGARD AR-138, 1979

[45] Compendium of Unsteady Aerodynamic Measurements, AGARD Advisory Report No. 702, 1982

[46] Schmitt, V. and F. Charpin, "Pressure Distributions on the ONERA-M6-Wing at Transonic Mach Numbers," Experimental Data Base for Computer Program Assessment Report of the Fluid Dynamics Panel Working Group 04, AGARD AR 138, May 1979.

[47] Yee, H., C., A Class of High-Resolution Explicit and Implicit Shock-Capturing Methods NASA Technical Memorandum 101088, Ames Research Center, Moffet Field, CA, Von Carman Institute for Fluid Dynamics, Lecture Series 1989-04.